Preprints of the 21st IFAC World Congress (Virtual)
Berlin, Germany, July 12-17, 2020

Dynamic In-Hand Regrasping Using a High-Speed Robot Hand and High-Speed Vision

Ryosuke Higo * **Taku Senoo** * **Masatoshi Ishikawa** *

* *the Dept. of Information Physics and Computing, Graduate School of Information Science and Technology, University of Tokyo, Tokyo 113-8656, Japan, (e-mail: ryosuke_higo@k2.t.u-tokyo.ac.jp).*

Abstract: This paper presents a robust and high-speed in-hand regrasping strategy on a two-dimensional plane. The proposed strategy features dynamic motion using a non-contact state with fingers. We used a pair of two-degrees-of-freedom fingers of a high-speed multi-fingered hand and a high-speed vision system. The proposed regrasping strategy consists of three phases: rotating, releasing, and catching. In all phases, visual information captured using a high-speed camera was used. The target state is the state in which the object is rotated 90° from the initial state. Experiments were conducted with different initial grasp positions for three cubes with different diameters and masses. In the experiments, 60 regraspings were performed. We achieved a 100% success rate (60/60). Each regrasping was completed in less than 0.2 s, and the results confirmed that the proposed approach represents a robust and high-speed regrasping strategy.

Keywords: Intelligent robotics, Robotics technology, Robots manipulators, Manipulation, Vision

1. INTRODUCTION

In-hand manipulation is an important skill for realizing dexterous manipulation. Several studies have focused on controlling the position and orientation of a grasped object. Dynamic control of the position and orientation of the object in the two-dimensional plane is realized by using rolling contact between the fingertip and object while maintaining a stable grasp in Arimoto et al. (2001), Ozawa et al. (2005). A few studies also investigated controlling the position of objects via underactuated grippers and visual servos in Calli and Dollar (2016). In the studies, the initial grasping state is crucial because the contact state is maintained. In the cases where the target grasp state is not achievable from the initial grasp state, it is necessary to perform regrasping to change the contact point between the fingertip and object. In many cases, regrasping changes the contact point of the fingertip with multiple fingers while maintaining a stable grasp. Therefore, it is difficult to realize fast regrasping with a stable grasp. In dynamic regrasping, fast regrasping is realized via throwing an object into the air and then catching it Furukawa et al. (2006). However, the success rate is 35% because the timing of catching is critical. Dynamic regrasping strategy is proposed even for a hand with low degree of freedom in Dafle et al. (2014), Shi et al. (2017), and Sintov and Shapiro (2018). In this case, extrinsic dexterity including inertia of an object, gravity, external contacts, and dynamic arm motions are used.

In previous studies, a fast and robust regrasping method using a dexterous robotic hand is not proposed. Therefore, in the present study, we realize fast and robust regrasping using a non-contact state that cannot be realized by manipulation using a contact state. The task for the dynamic in-hand regrasping involves rotating an object by 90 °. As shown in Fig. 1, the regrasping consists of three phases, namely rotating, releasing, and catching. The strategy uses intrinsic dexterity and extrinsic dexterity. For intrinsic dexterity, a robotic hand rotates an object by using the fingertips. For extrinsic dexterity, object inertia is used after releasing, and a table is used to generate a two-dimensional motion. The regrasping strategy is challenging because failures easily occur as shown in Fig. 2. In rotating, if a translational motion occurs, catching fails because the object can move away from the finger's reachable area. After being released, the object can contact with a finger again because the object is rotating rapidly. This leads to a large translational motion. Catching can fail because of sensing delay and low responsivity of fingers. In Furukawa et al. (2006), visual feedback was used only in the catching phase where the non-contact state occurs. In the study, in order to deal with objects with different initial positions and masses, diameters, and friction, we additionally use visual feedback in rotating and releasing to realize the robust and fast regrasping of the object because its parameters change. It is difficult to generate a trajectory in advance because rolling contact is used for rotating. Therefore,

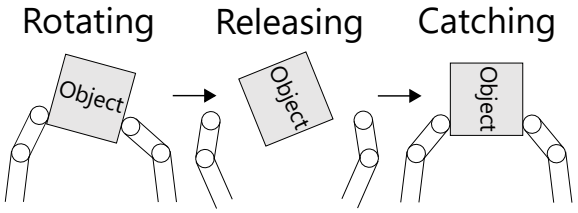

Fig. 1. Dynamic in-hand regrasping.

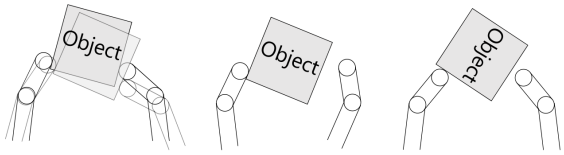

(a) Rotating failure. (b) Releasing failure. (c) Catching failure

Fig. 2. Possible failure in dynamic in-hand regrasping.

we obtain the rotation of the object with a high-speed vision device and generate the fingertip trajectory in real-time. At the moment of release, the system instantaneously changes from a grasping state to a non-grasping state wherein the two fingers must simultaneously leave the object. A possibility of a large translational motion exists in the object if the release timing of either of the two fingers is delayed and in contact with the object. Therefore, to realize an instantaneous releasing operation, the release timing is controlled via the high-speed vision device, response characteristics of the joints of the high-speed robot hand are adjusted, and high-performance response of the hand is utilized. During the catching action, the motion of the object after releasing is obtained by the high-speed camera and catching position and timing are controlled via visual feedback.

In Higo et al. (2018),regrasping using a high-speed vision device solely to control the timing of the catching operation is realized while handling a Rubik's cube. However, the joint trajectory is constant, and theoretical derivation of the kinematics of rolling between the object and fingertip is not been done. Therefore, it is necessary to derive kinematics to deal with various objects and to confirm its effectiveness in experiments.

In the study, we first solve forward kinematics and inverse kinematics with rolling contact such that we can determine the angular velocity of the joint when the motion of the object is given. Subsequently, we propose a strategy for regrasping at high-speed by inducing angular velocity to the object using the aforementioned inverse kinematics. We then conduct experiments on three cubes using a high-speed robot hand and confirm the effectiveness of the proposed strategy.

2. FORWARD KINEMATICS AND INVERSE KINEMATICS WITH ROLLING CONTACT

In a previous study, the kinematics of the spin-rolling motion of rigid objects is derived(Cui and Dai (2010)) and forward kinematics and inverse kinematics of velocity with rolling contact are derived (Cui et al. (2017)). The study does not derive kinematics where the finger exhibits two degrees of freedom and hemisphere. In this section, we solve the forward and inverse kinematics for the velocity in the case where the fingertip and object are in rolling contact. Hence, it is possible to obtain the velocity of each joint given the velocity of the object.

2.1 Forward kinematics

As shown in Fig. 3, the homogeneous transformation matrix from the robot coordinate system R to the fingertip coordinate system F is g_{RF} and that from the robot coordinate system R to the contact coordinate system M is g_{RM}. The coordinate system M is the Darboux frame(Cui and Dai (2010)). The spatial velocity(Murray (1994)) of the object coordinate system O with respect to the robot coordinate system R(Cui et al. (2017)) is V^s_{RO}. Specifically, V^s_{RF}, V^s_{FM}, and V^s_{MO} denote the spatial velocity of R with respect to F, F to M, and M to O, respectively.

$$V^s_{RO} = V^s_{RF} + \mathrm{Ad}_{g_{RF}} V^s_{FM} + \mathrm{Ad}_{g_{RM}} V^s_{MO} \,. \tag{1}$$

Equation (1) is equivalent to the following:

$$\widehat{V}^s_{RO} = \widehat{V}_{RF} + g_{RF}\widehat{V}^s_{FM}g^{-1}_{RF} + g_{RM}\widehat{V}^s_{MO}g^{-1}_{RM} \,. \tag{2}$$

The $\wedge$ operator forms a matrix in $se(3)$ out of a given vector in $\mathbb{R}^6$(Murray (1994)). The angle of the object θ_{Obj} is positive in the counterclockwise direction as shown in Fig. 3 and is set to $0°$, and the angle between the fingertip and object is as follows:

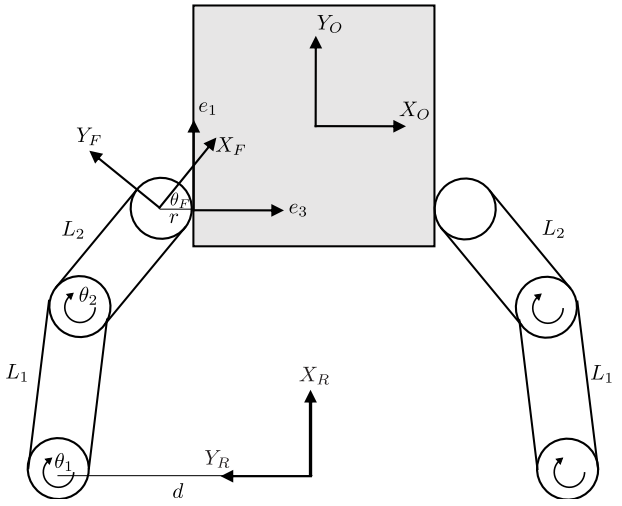

Fig. 3. Kinematics with rolling contact.

$$\theta_F = \theta_1 + \theta_2 + \theta_{\mathrm{Obj}} + (-1)^{n+1} \cdot 90 \,. \tag{3}$$

where $n = 0$ in the left finger and $n = 1$ in the right finger. We assume that the radius of the fingertip hemisphere is r and the rolling rate between fingertips and objects is σ(Cui and Dai (2010)), and equation (2) is expressed as follows:

$$\widehat{V}^s_{RO} = A \begin{bmatrix} \dot{\theta}_1 \\ \dot{\theta}_2 \\ \sigma \end{bmatrix} = \begin{bmatrix} A_1 & A_2 & A_3 \end{bmatrix} \begin{bmatrix} \dot{\theta}_1 \\ \dot{\theta}_2 \\ \sigma \end{bmatrix} \tag{4}$$

where

$$A_1 = \begin{bmatrix} -(-1)^n \cdot d \\ 0 \\ -1 \end{bmatrix}, A_2 = \begin{bmatrix} L_1 \sin(\theta_1) - (-1)^n \cdot d \\ L_1 \cos(\theta_1) \\ -1 \end{bmatrix} \tag{5}$$

$$A_3 = \begin{bmatrix} \frac{1}{r}\left(-L_2 \sin(\theta_2 + \theta_1) - L_1 \sin(\theta_1) + (-1)^n \cdot d\right) - S_{12F} \\ \frac{1}{r}\left(-L_2 \cos(\theta_2 + \theta_1) - L_1 \cos(\theta_1)\right) - C_{12F} \\ \frac{1}{r} \end{bmatrix} \tag{6}$$

where

$$S_{12F} = \sin(\theta_2 + \theta_1 - \theta_F) \,, \tag{7}$$

$$C_{12F} = \cos(\theta_2 + \theta_1 - \theta_F) \,. \tag{8}$$

2.2 Inverse kinematics

We assume that p_{RO} and R_{RO} denote the translation and rotation, respectively, of the object with respect to the robot coordinate system R. The spatial velocity of the object is expressed as follows:

$$V^s_{\mathrm{Obj}} = \begin{bmatrix} -\dot{R}_{RO}R^T_{RO}p_{RO} + \dot{p}_{RO} \\ \left(\dot{R}_{RO}R^T_{RO}\right)^\vee \end{bmatrix} = \begin{bmatrix} {}^R O_y\omega + {}^R\dot{O}_x \\ -{}^R O_x\omega + {}^R\dot{O}_y \\ 0 \\ 0 \\ 0 \\ \omega \end{bmatrix} . \tag{9}$$

The $\vee$ operator extracts the 6-dimensional vector that parameterizes a twist(Murray (1994)). Specifically, ${}^{R}O_x$ and ${}^{R}O_y$ denote the x and y coordinates, respectively, of the rotation center of the object, and ω denotes the angular velocity. Inverse kinematics solves $V^s_{RO} = V^s_{\mathrm{Obj}}$. Therefore, the solution of the inverse kinematics is expressed as follows:

$$\begin{bmatrix} \dot{\theta}_1 \\ \dot{\theta}_2 \\ \sigma \end{bmatrix} = A^{-1} \begin{bmatrix} {}^{P}O_y\omega + {}^{P}\dot{O}_x \\ -{}^{P}O_x\omega + {}^{P}\dot{O}_y \\ \omega \end{bmatrix} \tag{10}$$

where

$$\det A = -\frac{L_1}{r}(r\sin(\theta_2 - \theta_F) + L_2\sin(\theta_2)) \neq 0\ . \tag{11}$$

Therefore, the following equation must be satisfied:

$$r\sin(\theta_2 - \theta_F) + L_2\sin(\theta_2) \neq 0\ . \tag{12}$$

When $\det A \approx 0$, the configuration is a singular configuration in which the joint velocity significantly increases.

3. REGRASPING STRATEGY

In this section, as shown in Fig. 1, we explain the regrasping strategy consisting of three phases: rotating, releasing and catching.

3.1 Rotating

In the rotating phase, it is necessary that the grasped object rotates around the center of gravity (CoG) position and also exhibits fast angular velocity such that the objects do not stop rotating after releasing for less than 90 °. Therefore, the rotating strategy is to rotate the objects as fast as possible around the CoG position. The advantages of the strategy are that it does not need object dynamics model parameters (for e.g., friction and mass) and it is robust with respect to different model parameters because high-speed vision can obtain CoG position in real-time.

To induce angular velocity to the object, the translational velocity is set to 0: ${}^{P}\dot{O}_x = 0$, ${}^{P}\dot{O}_y = 0$ and equation (10) yields

$$\begin{bmatrix} \dot{\theta}_1 \\ \dot{\theta}_2 \\ \sigma \end{bmatrix} = \omega A^{-1} \begin{bmatrix} {}^{P}O_y \\ -{}^{P}O_x \\ 1 \end{bmatrix}\ . \tag{13}$$

It is difficult to control the target velocity because the velocity changes with the current joint angle and rotation of the object. However, the rotating strategy is feasible because an increase in ω increases the angular velocity. Specifically, ω is experimentally set such that the object rotates as fast as possible and translational motion does not occur. Thus, the two fingers can rotate the object while maintaining contact. Hence, θ_1, θ_2 is obtained from the robot hand's encoders at 1 ms and θ_{Obj}, ${}^{P}O_x$, and ${}^{P}O_y$ is obtained with the high-speed vision device at approximately 700 frame per second(fps).

3.2 Releasing

When $\theta_F > 65°$ in the rotating phase, both fingers are released from the object. When releasing, the fingers are simultaneously released and positioned away from the object. If the release timing differs between the left and right fingers, there is a possibility that a large translational motion can occur and the possibility of failure to catch the object increases. The response characteristics of each joint are adjusted, and simultaneous release is realized by utilizing the speed of the high-speed robot hand. The target joint angle of the left finger is $\theta_1 = -85°$, $\theta_2 = -85°$ and the target joint angle of the right finger is $\theta_1 = -85°$, $\theta_2 = \theta_{\mathrm{prev2}}$. Furthermore, θ_{prev2} is the value of the right finger joint angle θ_2 in the previous control cycle. The values are experimentally set such that the fingertip does not touch the object.

3.3 Catching

When the fingertip is released, the object performs the rotational motion. During the motion, position and orientation are obtained by the high-speed vision device. In the study, we perform regrasping to rotate the object by 90°. The catching position is controlled via visual feedback such that it is identical to the initial grasping position. Catching is performed at the moment when the angle of the object exceeds 70°. The target fingertip coordinates of the left finger are $(x_{init}, {}^{P}O_y + D/2)$ and those of the right finger are $(x_{init}, {}^{P}O_y - D/2)$. Specifically, D denotes the diameter of the object, and x_{init} denotes the fingertip coordinate that realizes the same contact point as the initial grasping position.

4. EXPERIMENT

4.1 System setting

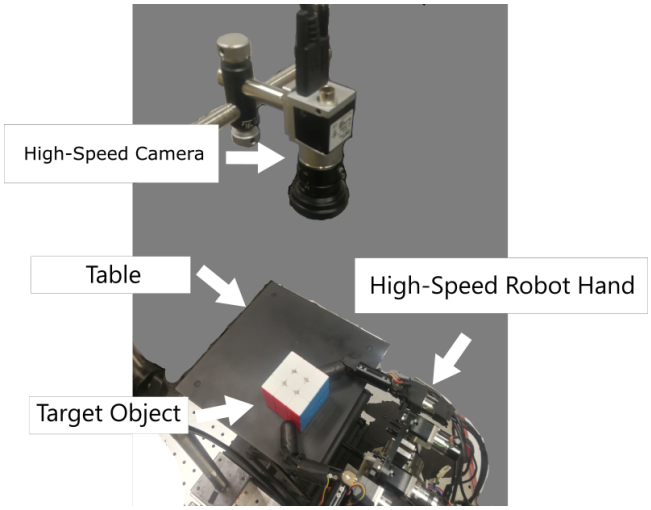

Fig. 4. Experiment system.

The experiment system is shown in Fig. 4. We use a high-speed multi-fingered hand (Namiki et al. (2003)). Two fingers with two degrees of freedom are used. The kinematics parameters in Fig 3 are $L_1 = 0.0635$ m, $L_2 = 0.0365$ m, $r = 0.0085$ m, and $d = 0.045$ m. In order to control the joint angle, joint velocity control is used in rotating and joint position control is used in releasing and catching. The control cycle is 1 ms. We placed an object on the table to generate motion in a two-dimensional plane. We use a high-speed camera, Basler ace 800-510uc, to obtain images of 528 px × 490 px at approximately 1000 fps After binarizing the obtained image, the center of gravity position and orientation of the object are calculated. The process is performed at approximately 700 fps.

We used three Rubik's cubes with different diameters and masses, as shown in Fig. 5, and we denote the objects as A,

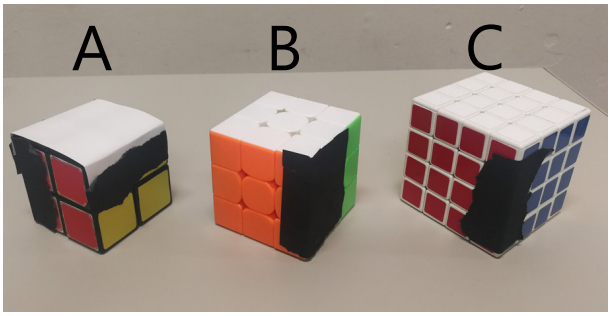

Fig. 5. Objects used for the experiments.

Table 1. Diameter and mass of the objects.

Object	Diameter[m]	Mass[kg]
A	0.0502	0.06
B	0.0555	0.08
C	0.0662	0.15

B, and C. The faces are fixed such that each face does not rotate. Each mass and diameter of the objects are as shown in Table 1. Only diameter information is set in advance. The position of the center of gravity is identical to the position of the geometric center of gravity of the square. The y coordinate of the initial position of the objects is ${}^{P}O_y = 0.00\,\mathrm{m}$ and the initial angle is $\theta_{\mathrm{Obj}} = 0^\circ$. The experiment was conducted via changing the x coordinate of the initial position. In the experiment, 60 regraspings (3 objects $\times$ 4 initial positions $\times$ 5) are performed. After grasping, the fingertip maintains contact with the objects, and the contact state is assumed as the point contact. We also use a low-friction table to rotate the objects on the table at a fast rate. The friction coefficient between the objects and table is not required because the fingertip trajectory is generated based on the rotation of the objects via high-speed visual feedback.

4.2 Result

As shown in Table 2, we conduct the regrasping experiments $E1$ to $E4$ in which the x coordinate of the initial center of gravity(CoG) position and initial grasp position are changed for objects A, B, and C. Experiments $E1$ to $E4$ are performed five times each for objects A, B, and C. We achieve a 100 % success rate(60/60), as shown in Table 3 and the regrasping time is less than 0.2 s in all experiments.

Table 2. Setting of experiments.

Experiment	Initial CoG position[m]	Initial grasp position[m]
E1	0.104	$0.104-0.018$
E2	0.095	$0.095-0.009$
E3	0.086	$0.086-0.000$
E4	0.076	$0.076+0.010$

Table 3. Result of experiments E1 to E4.

	Success rate[%]		
Experiment	*A*	*B*	*C*
E1	100 (5/5)	100 (5/5)	100 (5/5)
E2	100 (5/5)	100 (5/5)	100 (5/5)
E3	100 (5/5)	100 (5/5)	100 (5/5)
E4	100 (5/5)	100 (5/5)	100 (5/5)

A graph plotting the angles of objects A, B, and C in experiment $E1$ is shown in Fig. 6. The robot hand starts rotating operation from $t = 0.00\,\mathrm{s}$. An experiment $E1$ of objects A, B, and C is recorded with a 500 fps high-speed camera, and the captured images are shown in Fig. 9, Fig. 10, and Fig. 11. Figure 9 shows an image sequence of object A in experiment $E1$ captured at every 0.02 s, and the catching operation was completed in $t = 0.10\,\mathrm{s}$. Figure 10 and Fig.11 show image sequences of objects B and C in experiment $E1$ captured every 0.022 s, and the catching operation is completed in $t = 0.110\,\mathrm{s}$.

A graph plotting the x and y coordinates of objects A, B, and C in experiment $E1$ is shown in Fig. 7 and Fig. 8. It is observed that the center of gravity positions of the three objects moved in the same direction. Furthermore, it is observed that vibration at the center of gravity position occurs after the catching operation.

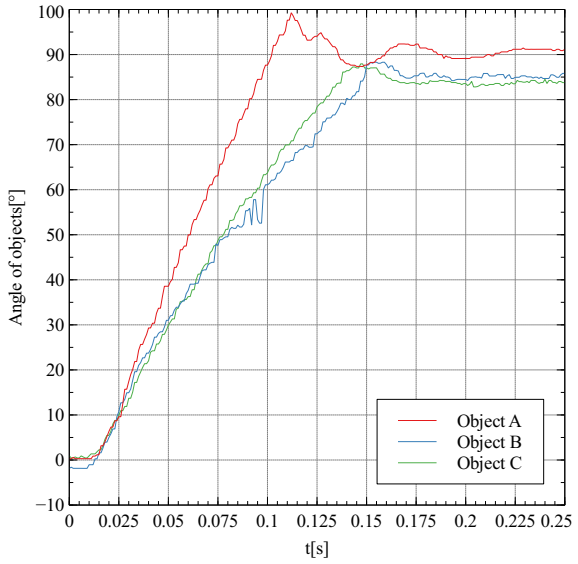

Fig. 6. Angle of objects in experiment $E1$.

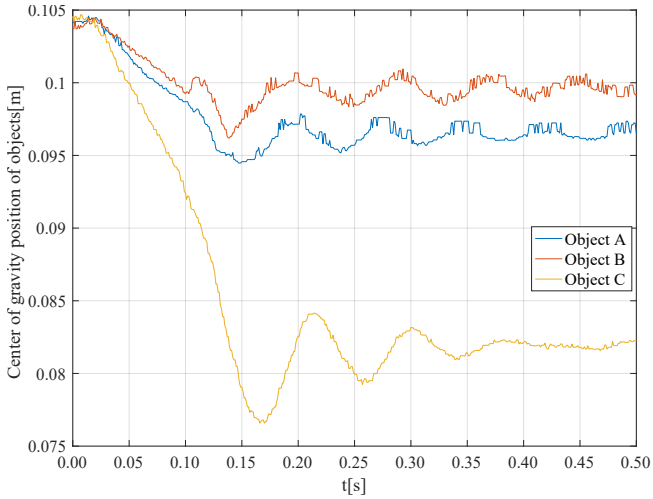

Fig. 7. x position of objects in experiment $E1$.

4.3 Discussion

The 100% success rate in all the experiments is achieved because the high-speed robot hand and the high-speed vision device are implemented for all phases and a delay is absent in the vision information. In Fig 6,7,8, each object trajectory is different due to differences in mass, diameter, and friction. The

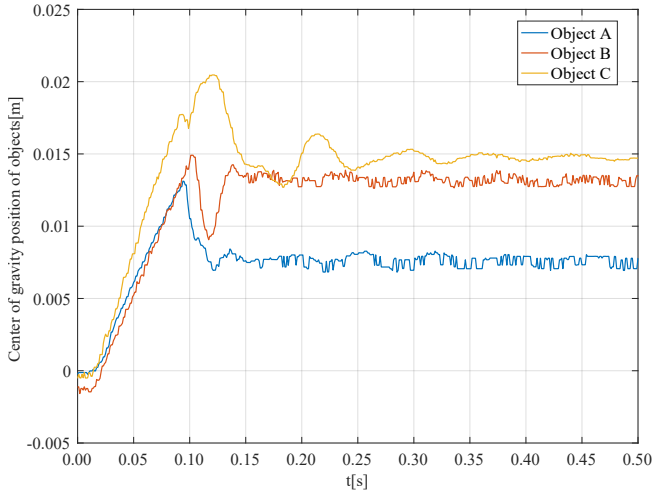

Fig. 8. y position of objects in experiment $E1$.

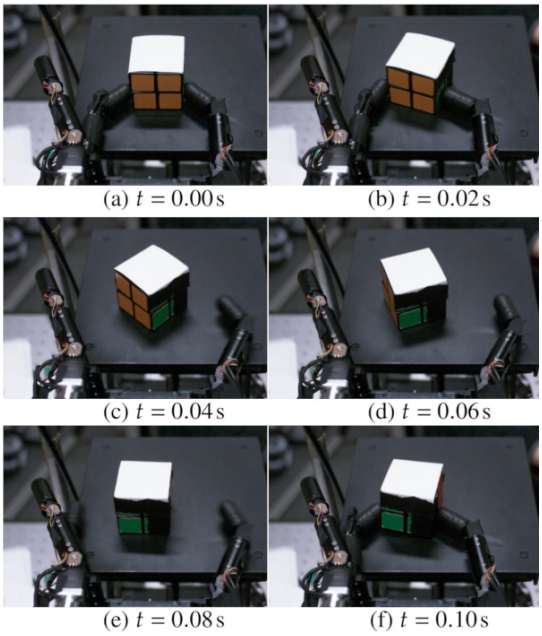

Fig. 9. Experiment $E1$ using object A.

regrasping strategy is robust for the objects without using the model parameters. Although the diameter is set in advance, it is obtained via the high-speed camera. Therefore, the proposed regrasping strategy is feasible without setting object parameters.

With respect to the fact that the position of the center of gravity moved after releasing although kinematics is considered, it is considered that the error is generated because modeling is not performed on the dynamics. The error is obtained with the high-speed camera, and the catching position was adjusted in real-time. With respect to the vibration of the center of gravity position after catching, it is considered that a strong shock occurs because the catching does not consider the impact and stops the rotating motion of the object in a moment.

Table 12 shows a comparison of similar regrasping strategies. Const denotes that visual information is not used in the phase. Timing denotes that it is used for a certain point in the phase when releasing or catching is performed. VisualFB denotes that

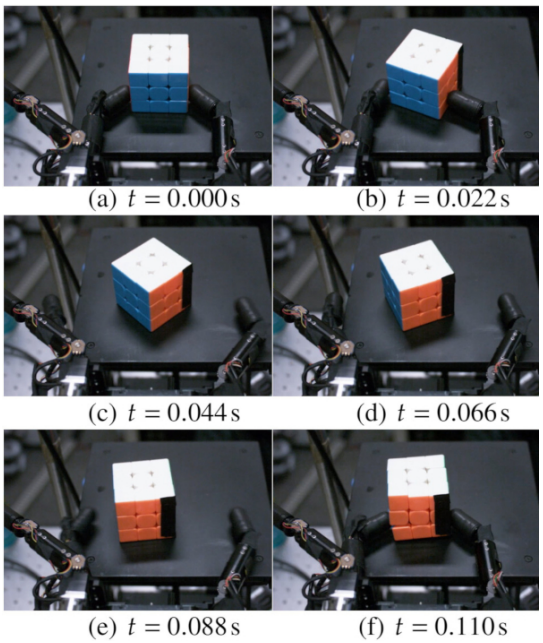

Fig. 10. Experiment $E1$ using object B.

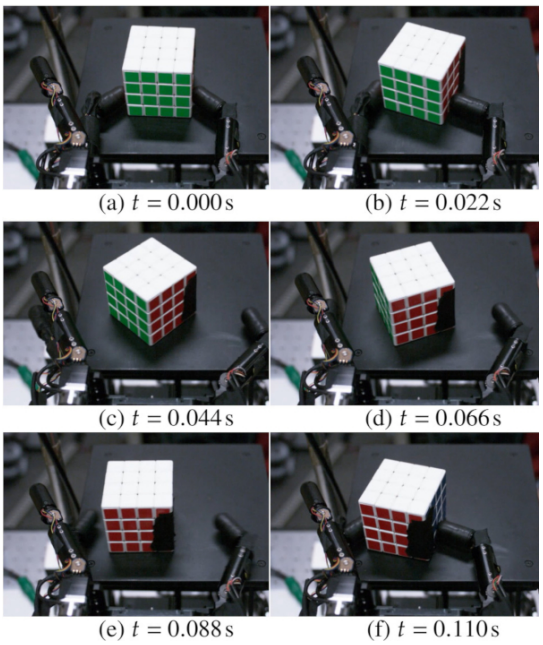

Fig. 11. Experiment $E1$ using object C.

Fig. 12. Comparison of use of vision

	Rotating	Releasing	Catching
Furukawa et al. (2006)	Const	Const	VisualFB
Higo et al. (2018)	Const	Const	Timing
Proposed	VisualFB	Timing	VisualFB

it is used for visual feedback. The proposed strategy is more adaptive than other strategies.

With respect to the condition in which the inverse matrix A^{-1} exists, when the left side of the equation (12) is 0, it becomes a singular configuration. In the system in the study, this occurs in the case shown in Fig. 13. When $\theta_F = 90°$, the value of θ_2 that satisfies the equation (12) is $\theta_2 = 7.62$. If $\theta_2 > 7.62$ during

rotation, it does not correspond to a singular configuration as shown Fig. 13. The graph plotting $\theta_2 = 7.62$ and left and right fingertip joint angles θ_2 in experiments $E1$ to $E4$ for objects A, B, and C are shown in Fig. 14. The left fingertip joint is in the range of $\theta_2 > -20$, and the right fingertip joint is in the range of $\theta_2 < -20$. A state exists where $\det A = 0$ occurs around $t = 0.030$ s. However, in all experiments, the rotating finishes by $t = 0.030$ s. Furthermore, given that it is almost impossible to realize the state of $\theta_F = 90°$ in the system, it is considered that a singular configuration did not occur.

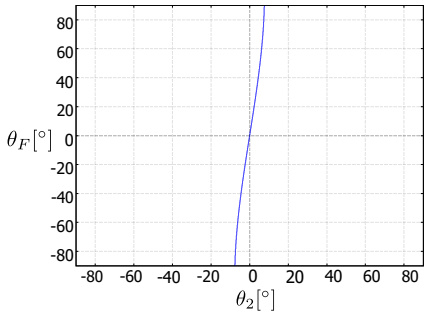

Fig. 13. Singularity of inverse kinematics with rolling contact.

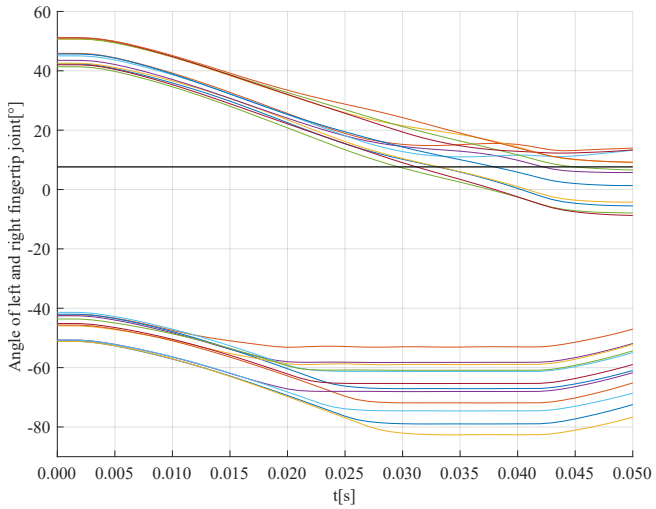

Fig. 14. Joint angle of the right and left fingertips.

5. CONCLUSION

In the study, to realize dynamic in-hand regrasping, we first solved the inverse kinematics for situations when the fingertip and object are in rolling contact. Subsequently, we proposed a regrasping strategy consisting of three phases: rotating, releasing, and catching. We then used a high-speed robot hand and a high-speed vision system to conduct regrasping experiments for three cubes of different diameters and different masses with different initial grasp positions. We achieved a 100% success rate of regrasping for all three objects. This was because the proposed strategy used visual information via high-speed vision in all phases. This was highly adaptive when compared to other strategies. Additionally, each regrasping time was less than 0.2 s. This was because the high-speed robot hand and the high-speed vision system can cope with the fast operation. Further experiments are required to determine the more accurate success rate.

It is considered that the study further enhanced the manipulation capability of the robot hand and is combined with other in-hand manipulation strategies such as positioning and orienting(Ozawa and Tahara (2017)).

A future task involves realization of regrasping for diverse objects such as those with a biased center of gravity position or objects with non-flat surface. Additionally, the timing of releasing and catching and its target joint angle were set experimentally, and thus it is necessary to develop a strategy that uses visual information to deal with diverse objects.

REFERENCES

Arimoto, S., Tahara, K., Yamaguchi, M., Nguyen, P.T.A., and Han, H.Y. (2001). Principles of superposition for controlling pinch motions by means of robot fingers with soft tips. *Robotica*, 19(1), 21–28.

Calli, B. and Dollar, A.M. (2016). Vision-based precision manipulation with underactuated hands: Simple and effective solutions for dexterity. *IEEE International Conference on Intelligent Robots and Systems*, 2016-Novem, 1012–1018.

Cui, L. and Dai, J.S. (2010). A darboux-frame-based formulation of spin-rolling motion of rigid objects with point contact. *IEEE Transactions on Robotics*, 26(2), 383–388.

Cui, L., Sun, J., and Dai, J.S. (2017). In-hand forward and inverse kinematics with rolling contact. *Robotica*, 35(12), 2381–2399.

Dafle, N.C., Rodriguez, A., Paolini, R., Tang, B., Srinivasa, S.S., Erdmann, M., Mason, M.T., Lundberg, I., Staab, H., and Fuhlbrigge, T. (2014). Extrinsic dexterity: In-hand manipulation with external forces. In *Proceedings - IEEE International Conference on Robotics and Automation*.

Furukawa, N., Namiki, A., Taku, S., and Ishikawa, M. (2006). Dynamic regrasping using a high-speed multifingered hand and a high-speed vision system. In *2006 IEEE International Conference on Robotics and Automation (ICRA)*, May, 181–187.

Higo, R., Yamakawa, Y., Senoo, T., and Ishikawa, M. (2018). Rubik's cube handling using a high-speed multi-fingered hand and a high-speed vision system. In *2018 IEEE/RSJ International Conference on Intelligent Robots and Systems (IROS)*, 6609–6614.

Murray, R.M. (1994). *A mathematical introduction to robotic manipulation*. CRC press.

Namiki, A., Imai, Y., Ishikawa, M., and Kaneko, M. (2003). Development of a high-speed multifingered hand system and its application to catching. In *Proceedings 2003 IEEE/RSJ International Conference on Intelligent Robots and Systems (IROS)*, volume 3, 2666–2671.

Ozawa, R., Arimoto, S., Nakamura, S., and Bae, J.H. (2005). Control of an object with parallel surfaces by a pair of finger robots without object sensing. *IEEE Transactions on Robotics*, 21(5), 965–976.

Ozawa, R. and Tahara, K. (2017). Grasp and dexterous manipulation of multi-fingered robotic hands: a review from a control view point. *Advanced Robotics*, 31(19-20), 1030–1050.

Shi, J., Woodruff, J.Z., Umbanhowar, P.B., and Lynch, K.M. (2017). Dynamic In-Hand Sliding Manipulation. *IEEE Transactions on Robotics*, 33(4), 778–795.

Sintov, A. and Shapiro, A. (2018). Dynamic regrasping by in-hand orienting of grasped objects using non-dexterous robotic grippers. *Robotics and Computer-Integrated Manufacturing*.